

## MINIMIZING THE DEFECT DENSITY OF MACROPOROUS SUPPORT COATINGS FOR MOLECULAR SEPARATION MEMBRANES

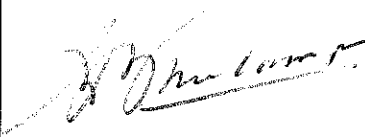

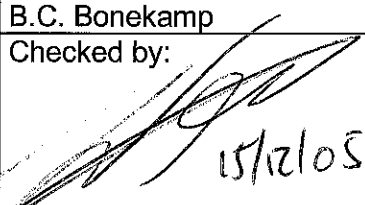
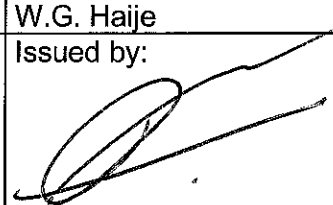
**B.C. Bonekamp**

**A. van Horsen**

**L.A. Correia**

**J.F. Vente**

*Presented at the International conference Porous Ceramic Materials (PCM2005),  
Brugge (Belgium). October 20-21, 2005*

Revisions		
A	10 October 2005, draft version	
B	14 December 2005; final version	
Made by:  B.C. Bonekamp	Approved by:  W.G. Hajje	ECN Energy Efficiency in Industry
Checked by:  J.F. Vente	Issued by:  P.T. Alderliesten	

December 2005

## Acknowledgements

Financial support from the EET METEOR project (EETK0157) and EET-KIEM 01009/4800000255 project is gratefully acknowledged.

## Abstract

Bubble number porometry and Hg porosimetry were used to investigate the density and size of percolating channels in gross macroporous support tubes, support tubes coated with one or two macroporous  $\alpha$ -alumina layers and the latter coated with a thin mesoporous  $\gamma$ -alumina layer. The key factor in obtaining macroporous thin layers with bulk properties is found in the application of multiple layers rather than the use of a single thicker layer. The breakthrough pressure of the layered macroporous substrate system increases drastically only when two coatings are applied with sufficient total thickness to shield larger voids. The bubble percolation behaviour of a mesoporous  $\gamma$ -alumina coating is determined by the width of the Hg intrusion curve of the underlying macroporous substrate coating(s). The mean macropore diameter is sufficiently low for depositing a sol-gel layer by colloidal filtration. However the largest pores in the distribution cause percolating channels in this layer. Hence the bubble point size/ mean pore size ratio of the  $\gamma$ -alumina coating is still  $\gg 1$  and needs to be improved by applying one or more macroporous coatings where the large pore size of the distribution is smaller than 100 nm.

## Keywords

Membrane support, porometry, bubble point, defect size, percolation.

## Contents

List of figures	4
1. Introduction	5
2. Experimental	6
3. Results and Discussion	7
4. Conclusion	10
References	11

## List of figures

Figure 3.1	<i>Bubble number density curves of mesoporous 4-layer support system for the E/A1/A6/<math>\gamma</math> system and the improved C/A6/A6/<math>\gamma</math> system .....</i>	7
Figure 3.2	<i>Bubble number porometry results of C tubes coated with 1 or 2 A6 layers, sintered at either 1100°C or 1250°C, and 1 <math>\gamma</math>-alumina layer .....</i>	8
Figure 3.3	<i>Hg intrusion and extrusion curves of A6 bulk compacts sintered at different temperatures. The inset shows the normalized curves.....</i>	8
Figure 3.4	<i>Bubble number density curves of single and A6 coatings with different thicknesses .....</i>	9

## 1. Introduction

Supported microporous layers with pores smaller than 1 nm can be used as a molecular separation membrane (MSM) for the separation of gases or liquids (see e.g. [1,2]). The separating layer of such a membrane system is usually ~100 nm thick. In the case of perfect layers, the pore characteristics, such as pore size distribution, tortuosity, and connectivity, are the determining factor for the separation characteristics. These characteristics are further influenced by the physical chemical properties of the solid-fluid interfaces. The selectivity decreases when the layer is not perfect and pores are present that are much larger than the intrinsic pore size. These defect pores are formed during the dip-coating process, due to asperities, larger voids, and dust particles, or during the drying/consolidating stage, due to shrinkage and interaction with the substrate. It is obvious that the concentration of imperfections must be kept as low as possible. One of the requirements to obtain such a layer is a support structure that is smooth, flawless and homogeneous. Although the above is recognised in the membrane literature no quantitative information in this respect can be found. In this paper, we will show that a substantial decrease in the defect population of mesoporous  $\gamma$ -alumina substrates for molecular separation membranes can be achieved by improving the macroporous layer system. Further, we will show that the key factor in obtaining thin layers with bulk properties is found in the application of multiple layers rather than the use of a single thicker layer.

## 2. Experimental

Coarse commercial macroporous substrate tubes (coded C) and in-house developed tubes (coded E) were used in the experiments. The porosity and d50 pore size of the C and E tubes are 0.43, 3.4  $\mu\text{m}$  and 0.35, 4.2  $\mu\text{m}$  respectively. The outer surface of the C tubes is about twice as smooth as that of the E tubes as measured with a mechanical profilometer.

High purity alumina powders (coded A1 and A6) were used for the preparation of coatings by colloidal processing [3]; suspensions were prepared by mixing and deagglomerating powder in an attritor, using a deflocculant. The A6 powder has a narrow primary particle size distribution (0.4-0.6  $\mu\text{m}$ ) and a specific surface area of 4-6  $\text{m}^2/\text{g}$ . The A1 powder has a specific surface area of  $\sim 3 \text{ m}^2/\text{g}$  and a bimodal size distribution in the range 2.5-9  $\mu\text{m}$ . The powders were calcined for 2h at 600°C before use.

After carefully drying the coated tubes were heated to 1100-1300°C for 2 hours followed by cooling down to 50°C. The layer thickness of the coating was calculated from coat mass and the porosity obtained from Hg-porosimetry.  $\alpha\text{-Al}_2\text{O}_3$  bulk compacts were prepared by quickly drying a few ml of suspension at 70°C, followed by sintering analogous to the respective coatings.

HCl peptised Boehmite sols were synthesised following the procedure of Leenaars [4] and Yoldas [5], using P.A. grade aluminium secondary butoxide, HCl, and Milli Q water.

Boehmite coatings were applied on the  $\alpha\text{-Al}_2\text{O}_3$  substrates in a clean room by colloidal filtration (see e.g. [2]). After ambient drying the coating was calcined for 2 hours at 600°C. Heating and cooling rate was 50°C/h.

Hg intrusion curves were recorded with a Micromeretics Autopore type II 9220. In order to compare Hg-porosimetry data with bubble porometry data it is convenient to define the void curvature  $J$  as follows:

$$J = \frac{\Delta P}{\gamma \cos \theta} = \frac{4}{d_L}, \quad (1)$$

Bubble porometry (see e.g. [6]) was done on tubes by closing one end and connecting the other end to a pressure controlled  $\text{N}_2$  supply. The tubes were wetted with pure water or ethanol by slowly immersing the tube into the liquid. On increasing the nitrogen pressure, the number of bubbles as function of the pressure is recorded until the number density was too large for bubble counting. We define the bubble breakthrough pressure as the extrapolation of the bubble density curve to zero bubble density.

### 3. Results and Discussion

Figure 3.1 shows the bubble porometry curves of the 4-layer support systems E/A1/A6/ $\gamma$  and C/A6/A6/ $\gamma$ . The highest density of the breakthrough curvature distribution in the population of E/A1/A6/ $\gamma$  tubes was about 10/ $\mu\text{m}$ . But the distribution was rather large. The highest curvature value incidentally observed was 20/ $\mu\text{m}$ . The bubble point curvature obtained for this system was always below that of the intrinsic pores of the  $\gamma$ -alumina layer (i.e.  $\sim 800/\mu\text{m}$ ). Above the bubble point the bubble number density increases rapidly with increasing curvature. The system C/A6/A6/ $\gamma$  has two macroporous  $\alpha$ -alumina A6 layers with both a thickness of about 40  $\mu\text{m}$ . The  $\gamma$ -alumina layer on this system now has a bubble point curvature J of about 25/ $\mu\text{m}$  having a small distribution. Beyond the bubble point a strong increase in bubble number density still occurs in the C/A6/A6/ $\gamma$ -alumina layer.

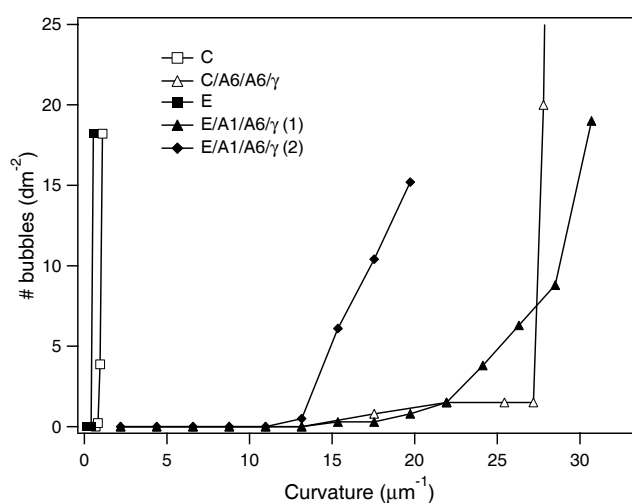


Figure 3.1 Bubble number density curves of mesoporous 4-layer support system for the E/A1/A6/ $\gamma$  system and the improved C/A6/A6/ $\gamma$  system

Figure 3.2 shows bubble porometry results of C/A6, C/A6/A6, C/A6/ $\gamma$  and C/A6/A6/ $\gamma$  substrate tubes. We found that the bubble point curvature of a single A6 coating of 40  $\mu\text{m}$  is about 1/ $\mu\text{m}$ . This is about the same value as the breakthrough curvature of the tube material. No significant shift in bubble point was observed in case of single A6 coatings. However, the slope of the curve decreases. A double (40  $\mu\text{m}$  + 40  $\mu\text{m}$ ) A6 coating appears to shift the bubble point curvature to about 22/ $\mu\text{m}$ . This is precisely the Hg breakthrough curvature of A6 bulk compacts of the same suspension (see Figure 3.3).

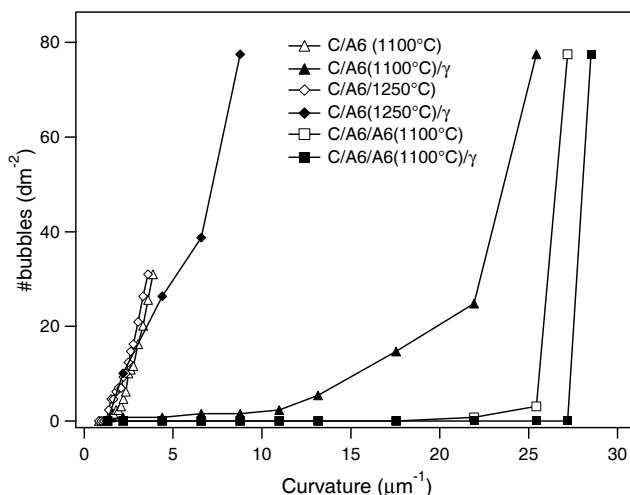


Figure 3.2 Bubble number porometry results of C tubes coated with 1 or 2 A6 layers, sintered at either 1100°C or 1250°C, and 1  $\gamma$ -alumina layer

After coating a  $\gamma$ -alumina layer on the improved C/A6(40  $\mu\text{m}$ )/A6(40  $\mu\text{m}$ ) system, we see only a slight shift in the bubble point curvature to higher values. When the pressure is increased beyond the bubble point a strong increase in bubble number density is observed. A  $\gamma$ -alumina coating on C/A6 results in a much lower slope of the bubble point curve (Figure 3.3) for C/A6(1100°C) but not for C/A6(1250°C).

The replacement of the coarse A1 layer by an A6 layer led to a macroporous A6 system showing bulk properties, i.e. having the same breakthrough point as a bulk A6 compact. The ratio breakthrough size/average A6 pore size is about 1.2 for the C/A6/A6 system and varies between 4 and 10 for the E/A1/A6 system. So the improvement is almost one order of magnitude. We observed that the breakthrough size of the gamma layer is always about the same as that of the macroporous substrate. However, the slope of the bubble density-curvature plot is lower. In this respect the changes between  $\gamma$ -alumina layers on the E/A1/A6/ $\gamma$  C/A6/A6/ $\gamma$  substrate are twofold: Almost no defects are present anymore larger than 0.2  $\mu\text{m}$  in the C/A6/A6/ $\gamma$   $\gamma$ -alumina system and the curvature where the bubble number density becomes higher than 100/dm<sup>2</sup> is shifted from a curvature of  $\sim 13/\mu\text{m}$  for the E/A1/A6/ $\gamma$  system to  $\geq 22/\mu\text{m}$  for the C/A6/A6/ $\gamma$  system.

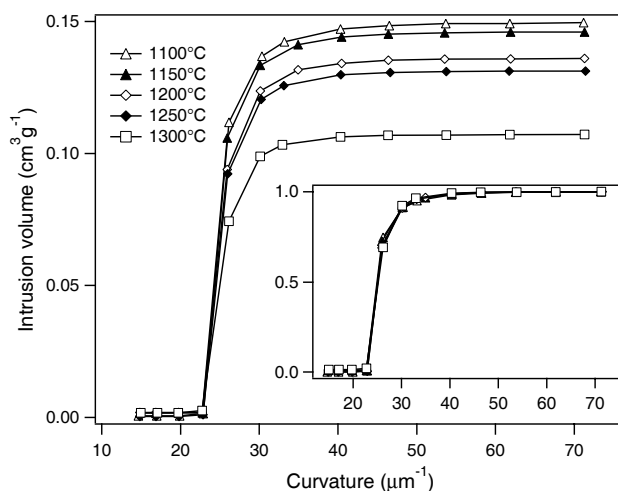


Figure 3.3 Hg intrusion and extrusion curves of A6 bulk compacts sintered at different temperatures. The inset shows the normalized curves



Note that the  $\gamma$ -alumina layer breakthrough size ( $\sim 180$  nm) of the C/A6/A6/ $\gamma$  system is still much larger than its average mesopore size of  $\sim 4$  nm [5,6], and hence the mesoporous layer can certainly not be considered as having bulk properties.

Figure 3.4 shows the effect of the layer thickness of single A6 coatings on the bubble number density curve and the effect of the thickness of the first and the second coating. We observed that a thicker single coating does not shift the bubble point curvature to higher values. Only lower slopes are observed. Coating first a thick and then a thin layer is not significantly better than a single coating of the same total thickness. However, coating first a thin layer and then a thicker one results in to a shift to higher bubble point curvature and a much larger decrease in slope.

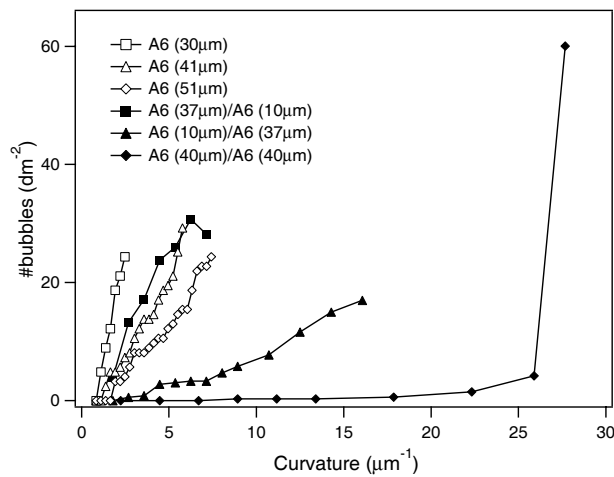


Figure 3.4 Bubble number density curves of single and A6 coatings with different thicknesses

## 4. Conclusion

We have shown that the bubble point curvature of single macroporous coatings is determined by the substrate tube properties. The breakthrough pressure of the layered A6 substrate system drastically increases when the coating is applied twice and the final thickness is sufficient to shield larger voids to approach "infinite size" percolation behavior. In that case the ratio bubble point curvature/bulk Hg intrusion curvature is close to 1. Further improvement with A6 powder is not possible. We showed that the bubble percolation behavior of a mesoporous  $\gamma$ -alumina coating is determined by the width of the Hg intrusion curve of the underlying substrate coating(s). The mean size of the A6 pores is sufficiently small for depositing a sol-gel layer by colloidal filtration. However, the large size pores of the distribution cause percolating channels in the mesoporous layer. The bubble point size/ mean pore size of the  $\gamma$ -alumina coating is still  $\gg 1$  and needs to be improved by applying one or more macroporous coatings having smaller percolating pores than can be obtained with the A6 powder. This can be achieved by using a finer sub-micrometer powder. These new insights will prove to be essential in the improvement of the reproducibility of microporous molecular separation membranes.

## References

- [1] Lin, Y.S. (2001): *Microporous and dense inorganic membranes: current status and prospective*. Sep.Pur.Technol., 25 (2001) 39.
- [2] Bonekamp, B.C. (1996): *Preparation of asymmetric ceramic membrane supports for pervaporation and gas separation membranes by dip coating*. Chapter 6 in: *Fundamentals of inorganic membrane science and technology*, Membrane Sci. Technol. 4 eds. A.J. Burggraaf and L. Cot., Elsevier, Amsterdam.
- [3] Lewis, J.A. (2000): *Colloidal processing of ceramics*. J. Am. Ceram. Soc., 83 (2000) 2341.
- [4] Leenaars, A.F.M., K. Keizer and A.J. Burggraaf (1984): *The preparation and characterisation of alumina membranes with ultra-fine pores*. Part 1. Microstructural investigations on non-supported membranes, J. Materials Sci., 19 (1984) 1077.
- [5] Yoldas, B.E. (1975): *Alumina gels that form porous transparent Al<sub>2</sub>O<sub>3</sub>*. J. Materials Sci, 10 (1975) 1856.
- [6] Jacobs, E. and W.J. Koros (1997): *Ceramic membrane characterization via the bubble point technique*. J. Membrane Sci., 124 (1997) 149.